

## Computation of Absorption Corrections on EDSAC II

By M. WELLS

*Crystallographic Laboratory, Cavendish Laboratory, Cambridge, England*

(Received 15 December 1959)

Programs are described for the computation of absorption corrections for single-crystal specimens of arbitrary shape; the programs have been applied to Weissenberg and Precession camera data and allow the specimen to be mounted in an absorbing cylindrical container.

### 1. Introduction

The need for accurate absorption corrections has long been realized and various authors in the past have described methods for dealing with weakly absorbing specimens (Frasson & Bezzi, 1959) or for evaluating corrections by hand computation (Rogers & Moffett, 1956; Albrecht, 1939). This paper deals solely with the methods used when a large high-speed computer is available and is an extension of the work of Busing & Levy (1957). The basis of the method is exactly as described in their work, with some minor modifications occasioned by the particular computer for which the programs were originally prepared. Only those arguments are described which lead to the determination of the direction cosines of the incident and emergent rays for different camera geometries, and the extension of the method to include cases where the specimen is mounted inside an absorbing cylindrical container, possibly with absorbing liquid trapped between one face of the crystal and the inner wall of the container.

### 2. Some basic reciprocal-lattice geometry

The problem is the determination of the direction cosines of the incident and reflected rays in some convenient axial set to which the crystal shape is also

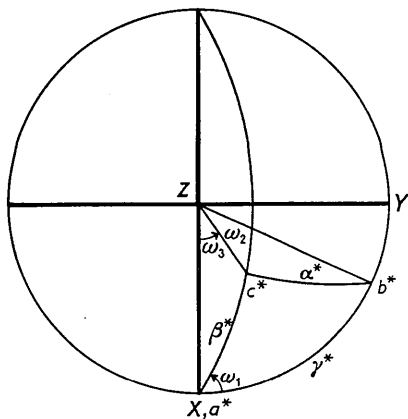


Fig. 1. Stereogram showing the relationship of the axes  $XYZ$  to the reciprocal lattice axes.

referred. We first define a right-handed orthogonal set of axes  $XYZ$  such that  $OX$  is coincident with  $a^*$ ,  $OY$  lies in the  $a^*b^*$  plane and  $c^*$  lies on the same side of  $OZ$  as the  $Y$  axis; in order to achieve this we may find it necessary to rename our crystallographic axes.

We shall find it convenient to work in terms of a number of intermediate angles  $\omega$ , and lengths in reciprocal space  $L$ , because any singularities in the behaviour of these intermediate variables can be detected in the course of the program by the computer which can then prevent anomalous results being produced. The angles  $\omega_i$  are measured anti-clockwise when viewed down  $OZ$  unless a statement to the contrary is made; lengths  $L$  are positive and square roots are taken as positive. Unless an explicit formula is given for a  $\left\{ \begin{smallmatrix} \sin \\ \cos \end{smallmatrix} \right\} \omega_i$  it is to be assumed that the expression

$$\left\{ \begin{smallmatrix} \sin \\ \cos \end{smallmatrix} \right\} \omega_i = \left( 1 - \left\{ \begin{smallmatrix} \cos \\ \sin \end{smallmatrix} \right\}^2 \omega_i \right)^{\frac{1}{2}}$$

is used.

The stereogram Fig. 1 shows the two sets of axes,  $a^*b^*c^*$  and  $XYZ$ ; in the figure all three reciprocal lattice axes are in the first quadrant but this is not essential. The angle  $\omega_1$  is given by

$$\cos \omega_1 = (\cos \alpha^* - \cos \beta^* \cos \gamma^*) / (\sin \beta^* \sin \gamma^*).$$

We can use the complement of  $\omega_1$  in  $a^*c^*Z$  to determine

$$\cos \omega_2 = \sin \omega_1 \sin \beta^*$$

and hence

$$\cos \omega_3 = \cos \beta^* / \sin \omega_2.$$

For  $\sin \omega_2$  to be zero we see that  $\beta^* \equiv \frac{1}{2}\pi$  in which case the expression for  $\cos \omega_3$  is indeterminate; such indeterminacy can readily be detected and the values  $\cos \omega_3 = 1$ ,  $\sin \omega_3 = 0$  substituted by the program.

The fact that  $\cos \omega_2$ ,  $\sin \omega_2$  and  $\sin \omega_3$  are all positive means that  $c^*$  must lie in the first or second quadrant.

Fig. 2 shows the reciprocal-lattice point  $hkl$ ,  $P$  and the two angles  $\omega_6$ ,  $\omega_7$  which specify the direction of the line joining  $P$  to the origin of the reciprocal lattice; this line is of course normal to the reflecting planes of which  $P$  is the representative point.

The length  $L_1$  gives the distance from the  $Z$ -axis

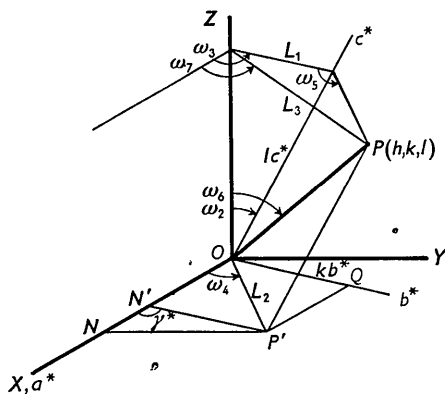


Fig. 2. The reciprocal lattice showing the angles and lengths referred to in section 2 of the text.

at which the  $c^*$ -axis intersects the  $l$ th layer of the reciprocal lattice and is given by

$$L_1 = lc^* \sin \omega_2 .$$

The length  $L_2$  gives  $OP'$ , the distance from the origin to the point  $hk0$  and has the value

$$L_2 = \{(ha^*)^2 + (kb^*)^2 + 2(ha^*)(kb^*) \cos \gamma^*\}^{\frac{1}{2}} .$$

Using  $L_2$  and the quantities

$$\begin{aligned} ON' &= ha^* \\ N'N &= kb^* \cos \gamma^* \\ NP' &= kb^* \sin \gamma^* \end{aligned}$$

we can evaluate  $\omega_4$  in the range  $0 \leq \omega_4 < 2\pi$  from

$$\begin{aligned} \cos \omega_4 &= (ha^* + kb^* \cos \gamma^*)/L_2 \\ \sin \omega_4 &= kb^* \sin \gamma^*/L_2 . \end{aligned}$$

The angle  $\omega_5$  is found from

$$\omega_3 + \omega_5 = \pi + \omega_4$$

so that

$$\cos \omega_5 = -\cos \omega_4 \cos \omega_3 - \sin \omega_4 \sin \omega_3$$

and this leads us to the value of  $L_3$ , given by

$$L_3 = \{L_1^2 + L_2^2 - 2L_1L_2 \cos \omega_5\}^{\frac{1}{2}} .$$

The length of the line joining  $P$  to the origin is  $2 \sin \theta$  where

$$2 \sin \theta = \{(ha^*)^2 + (kb^*)^2 + (lc^*)^2 + 2(kb^*)(lc^*) \cos \alpha^* + 2(ha^*)(lc^*) \cos \beta^* + 2(ha^*)(kb^*) \cos \gamma^*\}^{\frac{1}{2}}$$

and we can thus determine  $\omega_6$  in the range  $0 \leq \omega_6 \leq \frac{1}{2}\pi$  from

$$\sin \omega_6 = L_3/2 \sin \theta ;$$

we can also determine  $\omega_7$ , in the range  $0 \leq \omega_7 < 2\pi$  from

$$\begin{aligned} \sin \omega_7 &= (L_1 \sin \omega_3 + L_2 \sin \omega_4)/L_3 \\ \cos \omega_7 &= (L_1 \cos \omega_3 + L_2 \cos \omega_4)/L_3 \end{aligned}$$

and we have thus located the normal to the reflecting plane by a point in the upper hemisphere of our stereogram.

In the next three sections we proceed to determine the direction cosines of the incident and reflected rays for three widely used camera geometries. We do this by consideration of the physical conditions these rays must satisfy; two conditions which must always be satisfied are:

- (1) The incident ray  $I$ , the normal to the reflecting plane  $P$ , and the reflected ray  $R$  are coplanar and so will always lie on a great circle.
- (2) The angles  $P\hat{I}$  and  $P\hat{R}$  will always be equal to  $\frac{1}{2}\pi - \theta$  so that  $I$  and  $R$  will lie on a small circle of radius  $\frac{1}{2}\pi - \theta$  about  $P$ .

These two conditions alone are insufficient to determine the directions of the rays, and a third condition is always introduced by the particular type of camera in use, as described below.

### 3a. The equi-inclination camera

The extra condition in this case is that the angles  $Z\hat{I}$  and  $Z\hat{R}$  are equal, being in fact  $\frac{1}{2}\pi - \mu$  where  $\mu$  is the equi-inclination angle; this condition implies that  $I$  and  $R$  lie on a small circle of radius  $\frac{1}{2}\pi - \mu$  about  $Z$ , as shown in Fig. 3(a).

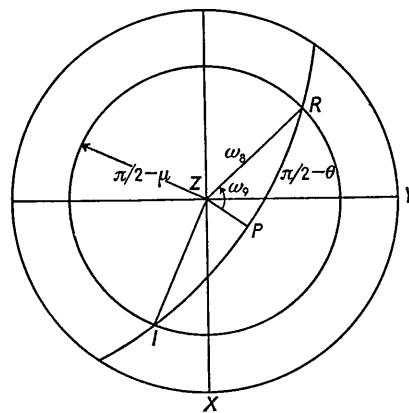


Fig. 3(a). The reflection geometry of the equi-inclination Weissenberg camera.

This, and the obvious symmetry of Fig. 3(a) such that the angle  $Z\hat{P}R = Z\hat{P}I = \frac{1}{2}\pi$  enable us to solve for

$\omega_8 = Z\hat{I} = Z\hat{R}$  in the range  $0 < \omega_8 \leq \frac{1}{2}\pi$  from

$$\cos \omega_8 = \cos \omega_6 \sin \theta ;$$

and we can then use this to solve for  $\omega_9$ , again in the range  $0 < \omega_9 \leq \frac{1}{2}\pi$ , from

$$\cos \omega_9 = (\sin \theta - \cos \omega_6 \cos \omega_8)/(\sin \omega_6 \sin \omega_8) .$$

We are now in a position to write down the direction

cosines of the incident and reflected rays which will be given by the following scheme:

$$\begin{aligned}\cos X^{\wedge} I &= \sin \omega_8 \{ \cos (\omega_7 - \omega_9) \} \\ &= \sin \omega_8 (\cos \omega_7 \cos \omega_9 + \sin \omega_7 \sin \omega_9) \\ \cos Y^{\wedge} I &= \sin \omega_8 \{ \cos (\frac{1}{2}\pi - \overline{\omega_7 - \omega_9}) \} \\ &= \sin \omega_8 (\sin \omega_7 \cos \omega_9 - \cos \omega_7 \sin \omega_9) \\ \cos Z^{\wedge} I &= \cos \omega_8 \\ &= \cos \omega_8 \\ \cos X^{\wedge} R &= \sin \omega_8 \{ \cos (\omega_7 + \omega_9) \} \\ &= \sin \omega_8 (\cos \omega_7 \cos \omega_9 - \sin \omega_7 \sin \omega_9) \\ \cos Y^{\wedge} R &= \sin \omega_8 \{ \cos (\omega_7 + \omega_9 - \frac{1}{2}\pi) \} \\ &= \sin \omega_8 (\sin \omega_7 \cos \omega_9 + \cos \omega_7 \sin \omega_9) \\ \cos Z^{\wedge} R &= \cos \omega_8 \\ &= \cos \omega_8\end{aligned}$$

### 3b. The normal-beam camera

The extra condition now is that the incident ray is always normal to  $OZ$  i.e. it lies on the primitive circle of the stereogram; there are now two possible positions for the incident ray, denoted by  $I, I'$  in Fig. 3(b), corresponding to reflections to the left and right hand side of the incident ray respectively (that is when viewed looking towards the source). The other possibility is that there are no intersections of the small circle and the primitive circle; this corresponds to a reflection which does not appear on a normal beam photograph.

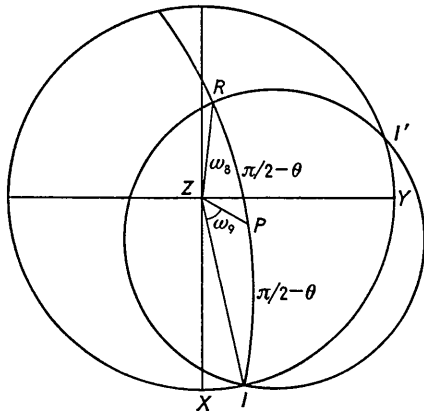


Fig. 3(b). The reflection geometry of the normal beam camera.

The angle  $IZP$  (which is not, in general, equal to  $R\hat{Z}P$ ) is given by

$$\cos \omega_9 = \sin \theta / \sin \omega_6$$

and this will be greater than 1 if no reflection is possible; this can be detected by the computer and appropriate action taken. The two sets of direction cosines for the incident beams  $I, I'$  are found from  $\omega_7 \pm \omega_9$  to be

$$\begin{aligned}\cos X^{\wedge} Y &= \cos (\omega_7 - \omega_9) \\ &= \cos \omega_7 \cos \omega_9 + \sin \omega_7 \sin \omega_9 \\ \cos Y^{\wedge} I &= \sin (\omega_7 - \omega_9) \\ &= \sin \omega_7 \cos \omega_9 - \cos \omega_7 \sin \omega_9 \\ \cos Z^{\wedge} I &= 0 \\ &= 0\end{aligned}$$

with corresponding expressions for  $I'$  obtained by reversing the sign of  $\omega_9$ .

The angle at  $P$  in the triangle  $IPZ$  is given by

$$\cos \hat{P} = \tan \theta \cot \omega_6 = (\sin \theta \cos \omega_6) / (\cos \theta \sin \omega_6)$$

and we can use the supplement of this angle in  $ZPR$  to evaluate  $\omega_8$  in the range  $0 < \omega_8 \leq \frac{1}{2}\pi$  from

$$\cos \omega_8 = \cos \omega_6 \sin \theta + \sin \omega_6 \cos \theta \cos \hat{P}$$

i.e.

$$\cos \omega_8 = 2 \cos \omega_6 \sin \theta.$$

This result will apply to both of the reflected beams and for a given value of  $l$  is independent of  $\theta$ , which we know to be the case; it is as convenient however to evaluate it afresh for each reflection. We can now solve for the angle  $P\hat{Z}R$  from

$$\cos \hat{Z} = (\sin \theta - \cos \omega_6 \cos \omega_8) / (\sin \omega_6 \sin \omega_8).$$

Now, from the values of  $\omega_7 \pm \hat{Z}$  we can form the direction cosines scheme for  $R$  and  $R'$ :

$$\begin{aligned}\cos X^{\wedge} R &= \sin \omega_8 \{ \cos (\omega_7 + \hat{Z}) \} \\ &= \sin \omega_8 (\cos \omega_7 \cos \hat{Z} - \sin \omega_7 \sin \hat{Z}) \\ \cos Y^{\wedge} R &= \sin \omega_8 \{ \cos (\omega_7 + \hat{Z} - \frac{1}{2}\pi) \} \\ &= \sin \omega_8 (\sin \omega_7 \cos \hat{Z} + \cos \omega_7 \sin \hat{Z}) \\ \cos Z^{\wedge} R &= \cos \omega_8 \\ &= \cos \omega_8\end{aligned}$$

with a corresponding set for  $R'$  found by reversing the sign of  $\hat{Z}$ .

The two positions for reflection correspond to two different spots on the film, or two different positions of the crystal and counter, and the absorption corrections for the two must be evaluated separately.

### 3c. The precession camera

The extra condition for the precession camera is that the incident beam lies on a small circle of radius  $\mu$ , the precession angle, drawn about  $Z$  the projection axis, as is shown in Fig. 3(c). It is also apparent from this that the anti-equi-inclination arrangement is a special case of the precession camera arrangement.

We can evaluate  $\cos \omega_{10}$  from

$$\cos \omega_{10} = (\sin \theta - \cos \omega_6 \cos \mu) / (\sin \omega_6 \sin \mu).$$

This may be greater than unity in certain situations corresponding to non-existent reflections; as before we

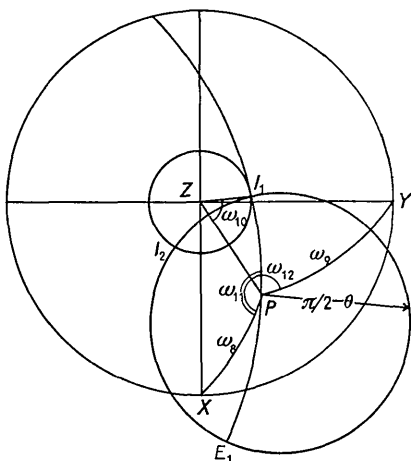


Fig. 3(c). The reflection geometry of the precession camera.

can detect these cases and prevent the production of 'corrections' for impossible reflections.

The use of  $\omega_7 \pm \omega_{10}$  enables us to evaluate the direction cosines of the incident rays  $I_1$  and  $I_2$ ; obviously

$$\cos Z \hat{I}_1 = \cos Z \hat{I}_2 = \cos \mu$$

and so

$$\begin{aligned} \cos X \hat{I}_1 &= \sin \mu \{ \cos (\omega_7 + \omega_{10}) \} \\ &= \sin \mu \{ \cos \omega_7 \cos \omega_{10} - \sin \omega_7 \sin \omega_{10} \} \end{aligned}$$

$$\begin{aligned} \cos Y \hat{I}_1 &= \sin \mu \{ \cos (\frac{1}{2}\pi - \overline{\omega_7 + \omega_{10}}) \} \\ &= \sin \mu \{ \sin \omega_7 \cos \omega_{10} + \cos \omega_7 \sin \omega_{10} \} \end{aligned}$$

$$\begin{aligned} \cos Z \hat{I}_1 &= \cos \mu \\ &= \cos \mu \end{aligned}$$

with a similar set for  $I_2$  found by reversing the sign of  $\omega_{10}$ .

To determine the direction cosines of the reflected rays we proceed by evaluating the direction cosines of the reciprocal lattice point  $P$ :

$$\cos X \hat{P} = \cos \omega_8 = \sin \omega_6 \cos \omega_7$$

$$\cos Y \hat{P} = \cos \omega_9 = \sin \omega_6 \sin \omega_7 .$$

Using these we can find the angles  $\omega_{11}$ ,  $\omega_{12}$  in Fig. 3(c);

$$\cos \omega_{11} = (\cos X \hat{I}_1 - \sin \theta \cos \omega_8) / (\cos \theta \sin \omega_8)$$

$$\cos \omega_{12} = (\cos Y \hat{I}_1 - \sin \theta \cos \omega_9) / (\cos \theta \sin \omega_9) .$$

The supplements of these angles lead to an expression

$$\begin{aligned} \cos X \hat{E}_1 &= \cos \omega_8 \sin \theta - \sin \omega_8 \cos \theta \cos \omega_{11} \\ &= 2 \cos \omega_8 \sin \theta - \cos X \hat{I}_1 \end{aligned}$$

and similar reasoning gives the scheme below for the direction cosines:

$$\cos X \hat{E}_1 = 2 \cos \omega_8 \sin \theta - \cos X \hat{I}_1$$

$$\cos Y \hat{E}_1 = 2 \cos \omega_9 \sin \theta - \cos Y \hat{I}_1$$

$$\cos Z \hat{E}_1 = -(1 - \cos^2 X \hat{E}_1 - \cos^2 Y \hat{E}_1)^{\frac{1}{2}}$$

with a similar set for the emergent ray.

These two sets of incident and reflected rays correspond now to the *same* reflection on the film, and the true correction to be applied is the arithmetic mean of the two separate corrections.

#### 4. The effect of absorbing specimen containers

If the specimen is mounted at the centre of a cylindrical container of dimensions large compared with those of the specimen then the effect of absorption in the container will be independent of position in reciprocal space and so for many purposes can be ignored.

A more usual situation is shown in Fig. 4, where the specimen is not at the centre of the container, and occupies an appreciable fraction of the total volume; in this case absorption by the container produces effects which depend on the direction of the reflection.

Suppose  $\mathbf{r}_0$  is a point on the axis of the cylinder, whose direction is specified by a unit vector  $\mathbf{t}$ ; the equation to the surface of the cylinder is

$$\{(\mathbf{r} - \mathbf{r}_0) \cdot \mathbf{t}\}^2 + a^2 = (\mathbf{r} - \mathbf{r}_0)^2 ,$$

where  $a$  is the radius of the cylinder.

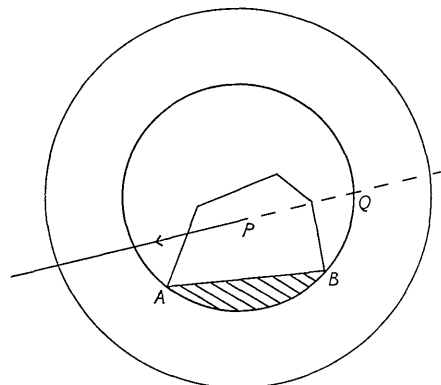


Fig. 4. Cross section of a crystal in an absorbing cylindrical container, with absorbing liquid between the face  $AB$  and the container.

A ray along the direction  $\mathbf{s}$  through a point  $\mathbf{r}_1$  within the specimen is

$$\mathbf{r} - \mathbf{r}_1 = k\mathbf{s}$$

and will intersect the cylinder at points where

$$\{(k\mathbf{s} + \mathbf{r}_1 - \mathbf{r}_0) \cdot \mathbf{t}\}^2 + a^2 = (k\mathbf{s} + \mathbf{r}_1 - \mathbf{r}_0)^2 .$$

This is a quadratic in  $k$ ;

$$\begin{aligned} k^2\{(\mathbf{s} \cdot \mathbf{t})^2 - 1\} + 2k\{\mathbf{s} \cdot \mathbf{t}(\mathbf{r}_1 - \mathbf{r}_0) \cdot \mathbf{t} - (\mathbf{r}_1 - \mathbf{r}_0) \cdot \mathbf{s}\} \\ + \{(\mathbf{r}_1 - \mathbf{r}_0) \cdot \mathbf{t}\}^2 - (\mathbf{r}_1 - \mathbf{r}_0)^2 + a^2 = 0 . \end{aligned}$$

There are two solutions to this equation, one with  $k$  negative, corresponding to the intersection of the

continuation of the ray and the cylinder as at  $Q$  in Fig. 4, and one with  $k$  positive; it is in this solution that we are interested. The actual path length of the ray within the container will be given by the difference between the two positive roots of the equations using the inner and outer radius; thus if

$$\begin{aligned} X &= (\mathbf{s} \cdot \mathbf{t})^2 - 1 \\ Y &= \{\mathbf{s} \cdot \mathbf{t}(\mathbf{r}_1 - \mathbf{r}_0) \cdot \mathbf{t} - (\mathbf{r}_1 - \mathbf{r}_0) \cdot \mathbf{s}\} \\ A_{i,o} &= \{(\mathbf{r}_1 - \mathbf{r}_0) \cdot \mathbf{t}\}^2 - (\mathbf{r}_1 - \mathbf{r}_0)^2 + a_{i,o}^2 \end{aligned}$$

the path length will be

$$k_o - k_i = \{(Y^2 - A_o X)^{\frac{1}{2}} - (Y^2 - A_i X)^{\frac{1}{2}}\} / X.$$

If there is an absorbing liquid trapped between one face of the specimen and the inner wall of the container then it becomes necessary to evaluate  $k_i$  and to subtract from this the path length within the crystal to the face to give the path length within the liquid; this need only be done for those rays which enter or leave by the face  $AB$ .

### 5. Discussion

The programs described above are all used to compute approximations to the value of the absorption correction by evaluating a weighted sum; it is of interest to know how accurate the approximation is and under what circumstances the method will fail.

The accuracy will naturally depend on how many sampling points are used, and it is perhaps worth noting that there are no limits to the accuracy other than those imposed by purely practical considerations — how long the computation would take and, more important, how accurately the size and shape of the crystal can be described. One limitation is that the crystal may not have re-entrant angles if the method of Busing & Levy is used for determining path lengths within the specimen. It has been found empirically

that by taking the integer next above  $4 \mu t$  in a given direction as the number of sampling points in that direction results are produced which agree to within ca. 3% of the true value, which can be evaluated analytically for certain special cases; this rule obviously fails where  $\mu t < 0.125$ ! The relative values of the corrections will, in general, be more accurate than their absolute values and except in work where absolute intensities are required it is the relative values which are important. A further check on accuracy has been made by measuring the changes in intensity when a crystal is rotated about the normal to the reflecting plane and comparing these with the changes in absorption correction; this work, carried out by Dr D. C. Phillips at the Royal Institution, is to form part of a separate publication.

The time per reflection increases approximately linearly with the product of the number of sampling points and the number of faces. A typical case, for 660 reflections, with 120 sampling points in a crystal with 6 faces, required 40 min. computer time.

I should like to thank Dr M. V. Wilkes of the Cambridge University Mathematical Laboratory for provision of computing facilities; Dr Wilkes has given permission for members of other laboratories to use EDSAC II for computing absorption corrections if they so desire and anyone wishing to avail himself of this offer should in the first instance write to me.

I am grateful to D.S.I.R. and the Royal Commission for the Exhibition of 1851 for financial support.

### References

- ALBRECHT, G. (1939). *Rev. Sci. Instrum.* **10**, 221.  
 BUSING, W. R. & LEVY, H. A. (1957). *Acta Cryst.* **10**, 180.  
 FRASSON, E. & BEZZI, S. (1959). *Acta Cryst.* **12**, 536.  
 ROGERS, D. & MOFFETT, R. H. (1956). *Acta Cryst.* **9**, 1037.